Piezoelectric properties of graphene oxide: A first-principles computational study

Zhenyue Chang, Wenyi Yan, Jin Shang, and Jefferson Zhe Liu

Citation: Applied Physics Letters **105**, 023103 (2014); doi: 10.1063/1.4890385
View online: http://dx.doi.org/10.1063/1.4890385
View Table of Contents: http://scitation.aip.org/content/aip/journal/apl/105/2?ver=pdfcov
Published by the AIP Publishing

Piezoelectric properties of graphene oxide: A first-principles computational study

Zhenyue Chang,[1] Wenyi Yan,[1] Jin Shang,[2] and Jefferson Zhe Liu[1,a)]
[1]*Department of Mechanical and Aerospace Engineering, Monash University, Clayton, Victoria 3800, Australia*
[2]*Department of Chemical and Biomolecular Engineering, The University of Melbourne, Victoria 3010, Australia*

(Received 6 April 2014; accepted 4 July 2014; published online 15 July 2014)

Some highly ordered compounds of graphene oxide (GO), e.g., the so-called clamped and unzipped GO, are shown to have piezoelectric responses via first-principles density functional calculations. By applying an electric field perpendicular to the GO basal plane, the largest value of in-plane strain and strain piezoelectric coefficient, d_{31} are found to be 0.12% and 0.24 pm/V, respectively, which are comparable with those of some advanced piezoelectric materials. An in-depth molecular structural analysis reveals that the deformation of the oxygen doping regions in the clamped GO dominates its overall strain output, whereas the deformation of the regions without oxygen dopant in the unzipped GO determines its overall piezoelectric strain. This understanding explains the observed dependence of d_{31} on oxygen doping rate, i.e., higher oxygen concentration giving rise to a larger d_{31} in the clamped GO whereas leading to a reduced d_{31} in the unzipped GO. As the thinnest two-dimensional piezoelectric materials, GO has a great potential for a wide range of micro/nano-electromechanical system (MEMS/NEMS) actuators and sensors. © *2014 AIP Publishing LLC*.
[http://dx.doi.org/10.1063/1.4890385]

Actuators have been adopted in a diverse range of micro/nanoelectromechanical systems (MEMS/NEMS), including medical devices,[1] microrobotic,[2] artificial muscle,[3–5] and many other smart structures.[6,7] There has been an immense effort towards the development of advanced actuation materials in the past decade. The extensively studied electromechanical actuation has several actuation schemes.[8,9] For example, the electrostatic force between charged objects can generate a mechanical motion, a piezoelectric strain is generated when piezoelectric materials are subject to an external electric field (i.e., the material remains charge neutral), and the electro-active actuation arises from electron or hole injection into electro-active materials (i.e., the material is charged). The piezoelectricity is widely used, because it exhibits a linear strain-electric field relation and a high response rate.[8–10] To be applied in NEMS, the dimension of piezoelectric materials should be reduced to a nanometer scale. Two-dimensional piezoelectric materials,[11–13] such as BN, MoS_2, $MoSe_2$, $MoTe_2$, WS_2, WSe_2, and WTe_2, are promising to address this demand. Graphene, as a representative of two-dimensional materials, have attracted a lot of interest because of its unique atomistic structure and excellent physical properties.[14–23] It is an ideal candidate for the design of two-dimensional piezoelectric materials.

Recently, Ong *et al*. used density functional theory (DFT) calculations to study the piezoelectric properties of graphene-based materials.[24] It is well known that the piezoelectric effect only exists in crystalline materials with no inversion symmetry. To break the inversion symmetry of pristine graphene, Ong *et al*. introduced adatom (e.g., Li, K, H, and F) onto the graphene surface. As a result, a maximum piezoelectric linear strain around 0.15% was generated.[24,25] However, the main drawback of their materials is the weak interactions between the adatom and graphene surface,[26] which may lead to desorption at a relatively high operation temperature or under a high actuation frequency, causing potential failures of materials and devices.[27]

Graphene oxide (GO), usually as the pre-product of synthesizing graphene, has generated huge interest for different types of applications.[28,29] The vast diversity of GO atomistic structures gives rise to different electronic and mechanical properties that are potentially useful for actuation material designing.[30–34] Recent experiments by Pandey *et al*. have shown highly ordered doping of oxygen (O) atoms on the hexagonal lattice of pristine graphene. Approximately 50% of the GO surfaces characterized using scanning tunneling microscope was found to comprise these periodic structures.[19] There are two possible O atom doping configurations: so-called clamped and unzipped (Fig. 1).[35] These two types of GO compounds break the inversion symmetry of pristine graphene, therefore inducing piezoelectricity in GO. For the unzipped GO, the oxygen atoms form strong covalent bonds to two neighboring carbon atoms as shown in Fig. 1(b). For the clamped GO (Fig. 1(a)), the calculated adsorption energy of oxygen atoms at the bridging sites is 4.8 eV, which is more than three times larger than that of Li, K, and H, and about two times higher than F.[26] In addition, the migration energy of oxygen on a graphene surface is about 1 eV, which is much higher than that of Li and K (e.g., 0.3 eV and 0.12 eV, respectively).[26] It is known that if the migration energy is less than 0.5 eV, the adatom is mobile on a graphene surface at room temperature.[26] The ease of bulk fabrication, diversity of atomistic structures, and good stability render GO compounds good candidates for two-dimensional piezoelectric materials.

a)Email: zhe.liu@monash.edu

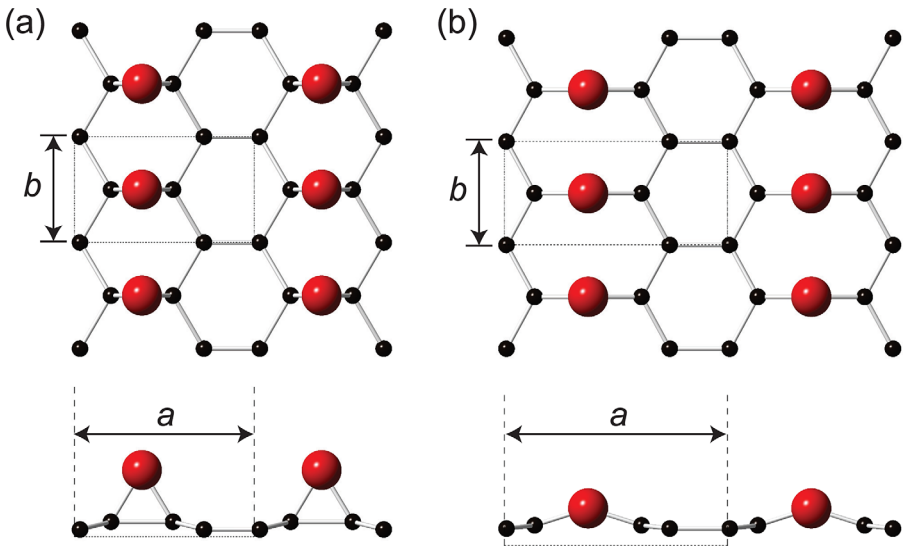

FIG. 1. Symmetrically clamped (a) and unzipped (b) GO configurations with a C/O ratio, $R_{C/O}$ of 4:1. Unit cells are depicted by dotted lines with in-plane lattice parameters shown as a and b. Black and red spheres represent the C and O atoms, respectively.

In this paper, we use first-principles calculations to investigate piezoelectric response of GO with different structural configurations. The obtained strain piezoelectric coefficients d_{31} are compared with results of the graphene with some physisorbed atoms. We also conduct an analysis to understand the structural origin of the piezoelectric strain in GO, which can explain the dependence of d_{31} on oxygen doping rate for the clamped and unzipped GO.

Figure 1 shows the unit cells of clamped and unzipped GO with a C/O ratio, $R_{C/O}$ of 4:1. For the unzipped GO, the C-C bond below oxygen atom is broken. Following the terminology from Xu and Xue, we term them as symmetrically clamped GO (sym-clamped) and symmetrically unzipped GO (sym-unzipped), respectively.[35] With the epoxy groups attached to one side, the crystal symmetry will be changed from a point group of *6/mmm* for pristine graphene to a non-inversion symmetric point group of *mm2*. In this study, the clamped GO crystals with a $R_{C/O}$ of 2 and 4 are examined. Our DFT calculations show that for $R_{C/O} > 4$, the clamped GO is unstable. For the unzipped GO crystals, a $R_{C/O}$ of 4, 8, or 16 is studied. It is found that an unzipped GO crystal with $R_{C/O} < 4$ is unstable.

The Vienna *ab initio* simulation package (VASP v.5.3.3) is used to perform density functional calculations on piezoelectric responses of symmetric GO. Projector augments wave pseudopotentials and the generalized gradient approximation are employed,[36,37] with a plane-wave cutoff energy of 800 eV. A Monkhorst-Pack gamma-centered k-points grid of dimensions $24 \times 42 \times 1$ is adopted for the C_2O-sym-clamped and C_4O-sym-clamped cells, while a $10 \times 40 \times 1$ is used for the C_8O-sym-unzipped GO cell. As periodic boundary conditions are employed in VASP, very thick vacuum layers are included to minimize interlayer interactions. An interlayer spacing of 20 Å is used throughout, which represents a good balance between computational accuracy and efforts.[38] To hold this interlayer space constant, the VASP source code is modified to allow the simulation cells to relax within the plane of GO, but not in the perpendicular direction.[39] In all cases, the C and O atoms are allowed to relax in all directions. Prior to being subjected to an external electric field, all structures are fully relaxed to determine their equilibrium lattice constants. The relative change of in-plane lattice constants under an applied electric field with respect to the equilibrium values are defined as piezoelectric strains.

Figure 2(a) shows the in-plane piezoelectric strains as a function of electric field strength from −0.5 to 0.5 eV/Å. A linear relation is observed for the sym-clamped GO crystals with $R_{C/O}$ of 2 and 4 and for the sym-unzipped GO crystals with $R_{C/O}$ of 4 and 8. Note that the magnitudes of the applied electric fields are experimentally achievable in graphene-based devices.[40] Overall, the sym-clamped GO has a better

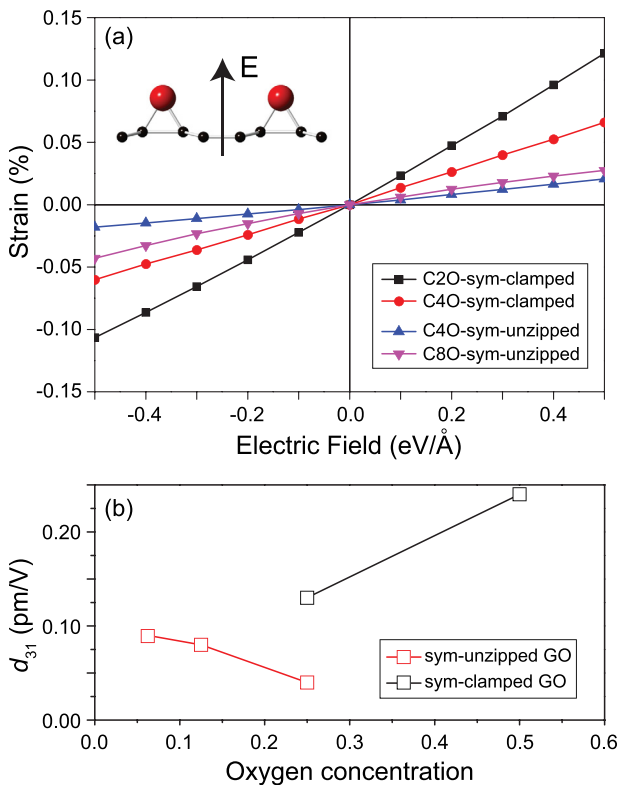

FIG. 2. (a) Piezoelectric strain of symmetric GO configurations being subject to an applied electric field perpendicular to the basal plane (inset). (b) The strain piezoelectric coefficient, d_{31} as a function of oxygen doping level for sym-clamped GO and sym-unzipped GO.

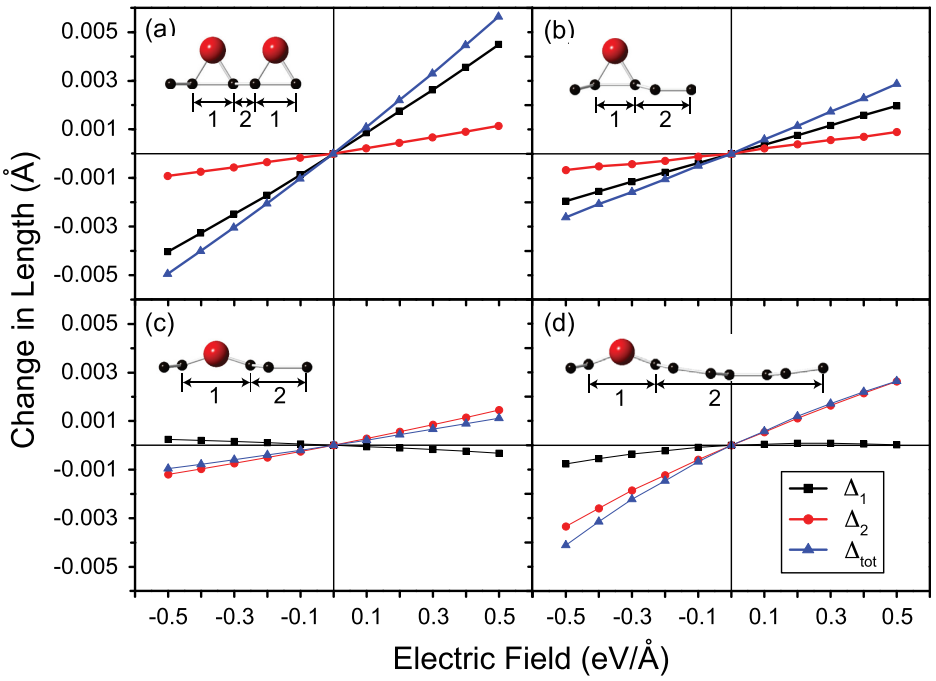

FIG. 3. Strain analysis of (a) C_2O-sym-clamped, (b) C_4O-sym-clamped, (c) C_4O-sym-unzipped, and (d) C_8O-sym-unzipped GO compounds. The change in total length, lengths of segment-1, and segment-2 of the supercells are represented by blue, black, and red symbols, respectively. Inset: side view of GO compounds with indications of segment-1 and segment-2. Black and red spheres represent the C and O atoms, respectively.

strain output than the sym-unzipped GO. The maximum strain output of 0.12% at an applied field of 0.5 eV/Å is close to the results from Ong *et al*. for graphene with some physisorbed adatoms (0.15%).[24]

Figure 2(b) shows that the strain piezoelectric coefficient, d_{31} (i.e., the slope of strain vs. electric field curve) as a function of oxygen concentration. Overall, the d_{31} coefficients for the clamped GO are significantly larger than those of the unzipped GO. A higher oxygen concentration in sym-clamped GO leads to a larger d_{31}, whereas an opposite trend is observed for the sym-unzipped GO. The C_2O-sym-clamped GO crystal has the maximum d_{31} (i.e., 0.24 pm/V), which is comparable with the maximum d_{31} coefficient obtained for the engineered piezoelectric graphene (i.e., 0.3 pm/V)[24] and the d_{31} coefficients of some three dimensional piezoelectric materials such as wurtzite boron nitride[41] and wurtzite GaN[42] (0.33 pm/V and 0.96 pm/V, respectively). But the d_{31} value is far smaller than the most widely used piezoelectric ceramics, Lead Zirconate Titanate (PZT), 119 pm/V.[43] It should be noted that for piezoelectric ceramic thin films with a thickness lower than 10 nm, the depolarization field generated by the accumulated surface charges will completely suppress the piezoelectric effects. Our proposed piezoelectric GO will not suffer this problem, giving rise to great potentials in NEMS applications.

To gain an in-depth understanding of piezoelectric properties of sym-clamped and sym-unzipped GO, we decomposed the in-plane deformation of GO crystals into two contributions. As shown in the insets of Fig. 3, the in-plane projection of interatomic distance of the two carbon atoms bonded by the oxygen atoms is defined as segment-1. The segment-2 is the in-plane projection of rest of the crystal. The total deformation, Δ_{tot} as shown in Fig. 3, is the summation of the length change in segment-1 and segment-2. For the sym-clamped cases (Figs. 3(a) and 3(b)), it is evident that the length change of segment-1, Δ_1 dominates the overall piezoelectric strain output. It appears that Δ_1 for C_2O-sym-clamped is almost twice of that of C4O-sym-clamped GO, which is consistent with increase of oxygen concentration (or the increase of portions of segment-1). The length change in segment-2, Δ_2 is approximately the same for the two clamped GO crystals. Thus, it is reasonable to understand that the strain output as well as the strain piezoelectric coefficient d_{31} is nearly doubled in C_2O-sym-clamped GO when comparing with the results of C_4O-sym-clamped GO (Fig. 2). In contrast, for the unzipped GO (Figs. 3(c) and 3(d)), Δ_1 is virtually negligible and the deformation mainly comes from segment-2. The increase of oxygen concentration reduces the proportion of segment-2 in the unzipped GO, thus leading to a reduction of d_{31} in Fig. 2(b).

With the oxygen concentration of GO reduced to 0.0625 (i.e., $R_{C/O} = 16$), some distinctive electromechanical properties were observed. Figure 4 shows the in-plane electromechanical strain as a function of the applied external electric

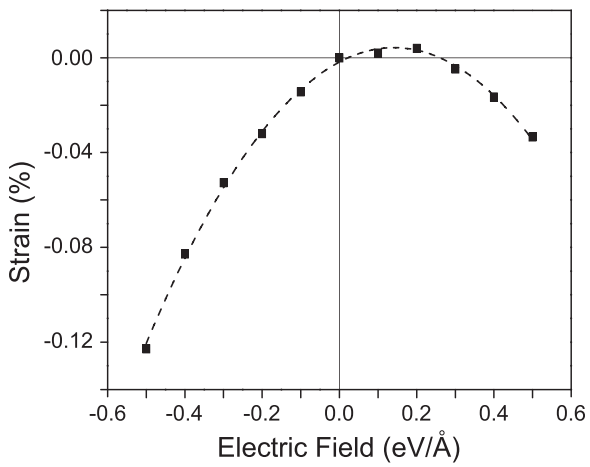

FIG. 4. In-plane strain of $C_{16}O$-sym-unzipped GO as a function of applied electric field perpendicular to the basal plane. The dashed line represents a second order polynomial fitting result.

field. It appears to be a parabolic relation with a clear shift toward the side of positive electric fields. We believe that the observed strain should originate from a combination of the electrostriction and piezoelectric effects. Fitting the nonlinear strain-electric field relationship using a second order polynomial yields $\varepsilon_{11} = -0.00303E_3^2 + 0.0009E_3 - 1.79 \times 10^{-5}$, in which ε_{11} is the in-plane strain and E_3 is the strength of electric field along the perpendicular direction. The linear term arises from the piezoelectric effect. The deduced coefficient $d_{31} = 0.09$ pm/V is shown in Fig. 2(b), which is consistent with the d_{31} results of other GO compounds. The electrostriction effect[44] shows $\varepsilon_{11} = M_{13}E_3^2$, from which the electrostriction coefficient M_{13} is determined as -3×10^{23} m^2/V^2. The results shown in Figure 4 indicate that the electrostriction dominates the electromechanical strains of $C_{16}O$-sym-unzipped GO. In contrast to most electrostrictive polymers, our GO crystal has a negative M_{13} coefficient. In other words, our $C_{16}O$-sym-unzipped GO crystal shows a contraction in the transverse direction upon the application of a perpendicular electrical field, whereas most electrostrictive polymers exhibit a transverse elongation. Physical origins for this distinctive electrostriction effect are not clear, which is worth of future investigations.

It is known that bulk materials without a band gap cannot exhibit piezoelectricity because a conductor is unable to produce sufficient electric polarization. Our DFT simulations show that only C_2O-sym-clamped and C_4O-sym-clamped GO have a band gap, i.e., 2.9 eV and 1.5 eV, respectively, whereas other compounds have a zero band gap. It appears that the observed piezoelectricity of our GO compounds with a zero band gap is contradictory to the well-accepted knowledge. However, it is worth to note that the GO crystals are only conducting in the basal plane of the sheet. Upon an applied electric field in the perpendicular direction to the basal plane, polarization can be induced and thus piezoelectricity can exist. This is a unique feature of two-dimensional materials, which is recognized by Ong *et al.*[24] Note that in VASP calculations, being subject to an electric field parallel to GO basal plane, indeed no piezoelectric effect is observed (i.e., $d_{11} = 0$). We also notice that the insulators (sym-clamped GO) have a larger d_{31} than the conductors (sym-unzipped GO) (Fig. 2(b)). But due to the limited results, it is hard to conclude this correlation.

In summary, piezoelectric properties of GO with different structural configurations and oxygen concentration are studied using the first-principles density functional calculations. The maximal values of in-plane strain and strain piezoelectric coefficient are obtained for C_2O-sym-clamped GO, i.e., a strain of up to 0.12% and $d_{31} = 0.24$ pm/V. An increase of oxygen concentration in the clamped GO enhances the piezoelectric strain output and the d_{31} coefficient, whereas an opposite trend is observed for the unzipped GO. Through an in-depth structural analysis, we find that the deformation of the oxygen-doped region dominates the piezoelectric strain of the clamped GO. On the contrary, deformation from the "graphene" region without oxygen dopant makes the major contribution to the piezoelectric strain of the unzipped GO. Interestingly, at a low oxygen concentration, the GO exhibits a much more profound electrostrictive deformation than the piezoelectric deformation. A negative electrostriction coefficient, M_{13}, is obtained for $C_{16}O$-sym-unzipped GO, in contrast to most of the electrostrictive polymers. Due to the excellent piezoelectric properties, the robust molecular structures, and an atomic thickness, GO crystals are promising two-dimensional piezoelectric materials for MEMS/NEMS actuators and sensors.

The authors acknowledge the Engineering Faculty of Monash University for providing a seed grant and acknowledge National Computational Infrastructure at Australian National University and Monash Sun Grid high-performance computing facility for providing the computational resources.

[1]J.-H. Jeon, T.-H. Cheng, and I.-K. Oh, "Snap-through dynamics of buckled IPMC actuator," Sens. Actuators, A: Phys. **158**, 300–305 (2010).
[2]S.-W. Yeom and I.-K. Oh, "A biomimetic jellyfish robot based on ionic polymer metal composite actuators," Smart Mater. Struct. **18**, 085002 (2009).
[3]G. W. Rogers and J. Z. Liu, "Monolayer graphene oxide as a building block for artificial muscles," Appl. Phys. Lett. **102**, 021903 (2013).
[4]J. Lu, S.-G. Kim, S. Lee, and I.-K. Oh, "A biomimetic actuator based on an ionic networking membrane of poly(styrene-alt-maleimide)-incorporated poly(vinylidene fluoride)," Adv. Funct. Mater. **18**, 1290–1298 (2008).
[5]R. H. Baughman, "Conducting polymer artificial muscles," Synth. Met. **78**, 339–353 (1996).
[6]U. Kim, J. Kang, C. Lee, H. Y. Kwon, S. Hwang, H. Moon, J. C. Koo, J.-D. Nam, B. H. Hong, J.-B. Choi, and H. R. Choi, "A transparent and stretchable graphene-based actuator for tactile display," Nanotechnology **24**, 145501 (2013).
[7]S.-E. Zhu, R. Shabani, J. Rho, Y. Kim, B. H. Hong, J. H. Ahn, and H. J. Cho, "Graphene-based bimorph microactuators," Nano Lett. **11**, 977–981 (2011).
[8]J. Z. Liu, G. W. Rogers, and J. Hughes, "Electromechanical actuation of pristine graphene and graphene oxide: Origin, optimization and comparison," in *Carbon Nanotubes for Actuators* (Springer, 2014).
[9]M. Tabib-Azar, *Microactuators* (Kluwer Academic Publishers, the Netherlands, 1997).
[10]C. R. de Lima, S. L. Vatanabe, A. Choi, P. H. Nakasone, R. F. Pires, and E. C. Nelli Silva, "A biomimetic piezoelectric pump: Computational and experimental characterization," Sens. Actuators, A: Phys. **152**, 110–118 (2009).
[11]K.-A. N. Duerloo, M. T. Ong, and E. J. Reed, "Intrinsic piezoelectricity in two-dimensional materials," J. Phys. Chem. Lett. **3**, 2871–2876 (2012).
[12]D. Wickramaratne, F. Zahid, and R. K. Lake, "Electronic and thermoelectric properties of few-layer transition metal dichalcogenides," J. Chem. Phys. **140**, 124710 (2014).
[13]H. J. Conley, B. Wang, J. I. Ziegler, R. F. Haglund, Jr., S. T. Pantelides, and K. I. Bolotin, "Bandgap engineering of strained monolayer and bilayer MoS_2," Nano Lett. **13**, 3626–3630 (2013).
[14]K. S. Novoselov, A. K. Geim, S. V. Morozov, D. Jiang, Y. Zhang, S. V. Dubonos, I. V. Grigorieva, and A. A. Firsov, "Electric field effect in atomically thin carbon films," Science **306**, 666–669 (2004).
[15]A. K. Geim, "Graphene: Status and prospects," Science **324**, 1530–1534 (2009).
[16]P. Avouris, Z. Chen, and V. Perebeinos, "Carbon-based electronics," Nat. Nanotechnol. **2**, 605–615 (2007).
[17]C. Lee, X. Wei, J. W. Kysar, and J. Hone, "Measurement of the elastic properties and intrinsic strength of monolayer graphene," Science **321**, 385–388 (2008).
[18]T. J. Booth, P. Blake, R. R. Nair, D. Jiang, E. W. Hill, U. Bangert, A. Bleloch, M. Gass, K. S. Novoselov, M. I. Katsnelson, and A. K. Geim, "Macroscopic graphene membranes and their extraordinary stiffness," Nano Lett. **8**, 2442–2446 (2008).
[19]D. Pandey, R. Reifenberger, and R. Piner, "Scanning probe microscopy study of exfoliated oxidized graphene sheets," Surf. Sci. **602**, 1607–1613 (2008).
[20]J.-A. Yan, L .Xian, and M. Chou, "Structural and electronic properties of oxidized graphene," Phys. Rev. Lett. **103**, 086802 (2009).
[21]R. H. Baughman, C. Cui, A. A. Zakhidov, Z. Iqbal, J. N. Barisci, G. M. Spinks, G. G. Wallace, A. Mazzoldi, D. D. Rossi, A. G. Rinzler, O. Jaschinski, S. Roth, and M. Kertesz, "Carbon nanotube actuators," Science **284**, 1340–1344 (1999).
[22]J. S. Bunch, A. M. van der Zande, S. S. Verbridge, I. W. Frank, D. M. Tanenbaum, J. M. Parpia, H. G. Craighead, and P. L. McEuen, "Electromechanical resonators from graphene sheets," Science **315**, 490–493 (2007).

[23]X. Xie, L. Qu, C. Zhou, Y. Li, J. Zhu, H. Bai, G. Shi, and L. Dai, "An asymmetrically surface-modified graphene film electrochemical actuator," ACS Nano **4**, 6050–6054 (2010).
[24]M. T. Ong and E. J. Reed, "Engineered piezoelectricity in graphene," ACS Nano **6**, 1387–1394 (2012).
[25]R. K. Prasad, *Quantum Chemistry* (New Age Science, Tunbridge Wells, 2010).
[26]K. Nakada and A. Ishii, "DFT calculation for adatom adsorption on graphene," in *Graphene Simulation* (InTech, Rijeka, 2011).
[27]M. Viefhues, S. Manchanda, T.-C. Chao, D. Anselmetti, J. Regtmeier, and A. Ros, "Physisorbed surface coatings for poly(dimethylsiloxane) and quartz microfluidic devices," Anal. Bioanal. Chem. **401**, 2113–2122 (2011).
[28]V. C. Tung, M. J. Allen, Y. Yang, and R. B. Kaner, "High-throughput solution processing of large-scale graphene," Nat. Nanotechnol. **4**, 25–29 (2008).
[29]G. Eda, G. Fanchini, and M. Chhowalla, "Large-area ultrathin films of reduced graphene oxide as a transparent and flexible electronic material," Nat. Nanotechnol. **3**, 270–274 (2008).
[30]J. W. Suk, R. D. Piner, J. An, and R. S. Ruoff, "Mechanical properties of monolayer graphene oxide," ACS Nano **4**, 6557–6564 (2010).
[31]J. Oh, M. E. Kozlov, J. Carretero-González, E. Castillo-Martínez, and R. H. Baughman, "Thermal actuation of graphene oxide nanoribbon mats," Chem. Phys. Lett. **505**, 31–36 (2011).
[32]D. W. Boukhvalov and M. I. Katsnelson, "Modeling of graphite oxide," J. Am. Chem. Soc. **130**, 10697–10701 (2008).
[33]G. W. Rogers and J. Z. Liu, "Graphene actuators: Quantum-mechanical and electrostatic double-layer effects," J. Am. Chem. Soc. **133**, 10858–10863 (2011).
[34]G. W. Rogers and J. Z. Liu, "High-performance graphene oxide electromechanical actuators," J. Am. Chem. Soc. **134**, 1250–1255 (2012).
[35]Z. Xu and K. Xue, "Engineering graphene by oxidation: A first-principles study," Nanotechnology **21**, 045704 (2009).
[36]G. Kresse and J. Furthmüller, "Efficient iterative schemes for *ab initio* total-energy calculations using a plane-wave basis set," Phys. Rev. B **54**, 11169–11186 (1996).
[37]G. Kresse and D. Joubert, "From ultrasoft pseudopotentials to the projector augmented-wave method," Phys. Rev. B **59**, 1758–1775 (1999).
[38]G. Sun, M. Kertesz, J. Kürti, and R. Baughman, "Dimensional change as a function of charge injection in graphite intercalation compounds: A density functional theory study," Phys. Rev. B **68**, 125411 (2003).
[39]VASP source code "*constr_cell_relax.F*" was modified in order to relax the *simulation supercell* in the GO basal plane only.
[40]Y. Zhang, T.-T. Tang, C. Girit, Z. Hao, M. C. Martin, A. Zettl, M. F. Crommie, Y. R. Shen, and F. Wang, "Direct observation of a widely tunable bandgap in bilayer graphene," Nature **459**, 820–823 (2009).
[41]K. Shimada, "First-principles determination of piezoelectric stress and strain constants of wurtzite III-V nitrides," Jpn. J. Appl. Phys., Part 2 **45**, L358–L360 (2006).
[42]A. Hangleiter, F. Hitzel, S. Lahmann, and U. Rossow, "Composition dependence of polarization fields in GaInN/GaN quantum wells," Appl. Phys. Lett. **83**, 1169 (2003).
[43]M. Dekkers, H. Boschker, M. van Zalk, M. Nguyen, H. Nazeer, E. Houwman, and G. Rijnders, "The significance of the piezoelectric coefficient $d_{31,eff}$ determined from cantilever structures," J. Micromech. Microeng. **23**, 025008 (2012).
[44]R. C. DORF, *The Electrical Engineering Handbook* (CRC Press, Inc., Boca Raton, 1997).